Electronic Supplementary Material (ESI) for Chemical Science.

Halogen bonded Borromean networks by design:
Topology invariance and metric tuning in a library of multi component systems

Vijith Kumar,[a] Tullio Pilati,[a] Giancarlo Terraneo,[a] Franck Meyer,[b] Pierangelo Metrangolo,[a,c] and Giuseppe Resnati*[a]

---

[a] *Laboratory of Nanostructured Fluorinated Materials (NFMLab)*
Department of Chemistry, Materials, and Chemical Engineering
“Giulio Natta”, Politecnico di Milano, Via L. Mancinelli 7, 20131 Milano, Italy
[b] *Present address: Laboratory of Biopolymers and Supramolecular Nanomaterials, Université Libre de Bruxelles, Boulevard du Triomphe, 1050 Bruxelles, Belgium*
[c] *VTT-Technical Research Centre of Finland, P.O. Box 1000, FI-02044 VTT, Finland*

Supplementary Information

Contents

S.1. Materials and methods

Commercial AR grade solvent (Ethanol) were used without any further purification for supramolecular synthesis and crystallization. Starting materials were purchased from Sigma–Aldrich, TCI (Europe and Japan) and Apollo Scientific. IR spectra were obtained using a Nicolet Nexus FT-IR spectrometer equipped with UATR unit. Melting points were determined with a Reichert instrument by observing the melting process through a polarizable optical microscope. DSC analysis were carried out with a Mettler Toledo DSC600 hot stage (10 °C/min). NMR spectra (^{1}H and ^{19}F) were recorded at ambient temperature on a Bruker AV-400 spectrometer, at 400 MHz. All chemical shifts are given in ppm. Ethanol-d_6 was used as a solvent.

S.2. Single crystal X-ray structure determination and data parameters

The crystals were diffracted using Mo-Kα radiation on a Bruker KAPPA APEX II diffractometer with a Bruker KRYOFLEX low temperature device. Crystal structures of the reported complexes were solved by direct method and refined against F^2 using SHELXL97 [1]. Packing diagrams were generated using Mercury 3.8. [2] Intermolecular interactions were analysed with PLATON. [3] The non-hydrogen atoms were refined anisotropically and hydrogen atoms were refined using difference Fourier map or positioned geometrically.

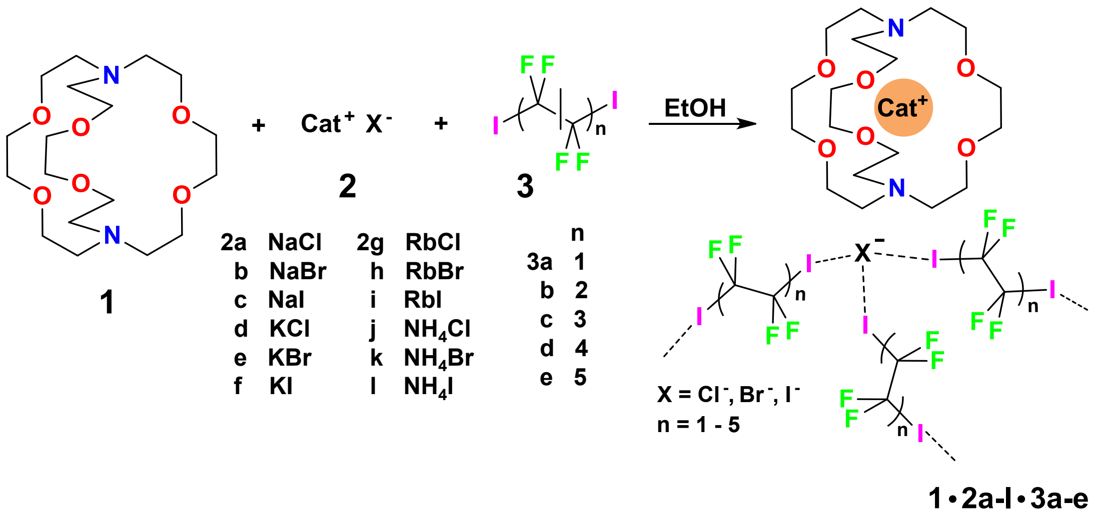

Table S.1. Crystallographic data and structure refinement parameters for cocrystals formed by crypt-222 (**1**), sodium chloride and bromide (**2a** and **2b**, respectively) and α,ω-diiodoperfluoroalkanes **3a-d**.

Structure	**1·2a·3a**	**1·2a·3b**	**1·2a·3c**
Formula	$C_{42}H_{72}Cl_2F_{12}I_6N_4Na_2O_{12}$	$C_{26}H_{36}ClF_{16}I_4N_2NaO_6$	$C_{54}H_{72}Cl_2F_{36}I_6N_4Na_2O_{12}$
Molecular formula	2(**1·2a**)·3(**3a**)	(**1·2a**)·2(**3b**)	2(**1·2a**)·3(**3c**)
Fw	1931.32	1342.61	2531.44
Crystallographic System	Trigonal	Orthorhombic	Monoclinic
Space group	*R*-3*c*	*C*222$_1$	***P***2$_1$
a (Å)	11.4435(9)	18.7124(17)	12.3140(12)
b (Å)	11.4435(9)	20.013(2)	22.647(2)
c (Å)	84.639(7)	11.7798(10)	15.5410(15)
α (°)	90	90.00	90.00
β (°)	90	90.00	92.803(10)
γ (°)	120	90.00	90.00
V (Å^3)	9598.8(13)	4411.4(7)	4328.8(7)
T (K)	103	103	103
Z	6	4	2
ρ (g.cm^{-3})	2.005	2.022	1.942
μ (mm^{-1})	3.099	3.001	2.354
Absorption correction T_{min}, T_{max}	0.4418, 0.5849	0.3972, 0.5101	0.6644, 0.7466
Collected, independent, obs. [$I>\sigma(I)$] reflections	154667, 6540, 5800	73501, 9047, 8147	63086, 28274, 23461
R_{int}	0.036	0.030	0.030
ϑ_{max}	39.99	35.28	33.42
Parameters, restraints	149, 39	323, 243	1268,1434
$wR(F^2)$, $R[F^2 > 2\sigma(F^2)]$	0.0564, 0.0246	0.0673, 0.0294	0.0863, 0.0383
Goodness of fit	1.103	1.084	1.010
Δρ (min,max)	-0.9,1.7	-0.6,1.2	-0.5, 1.9
Topology of supramolecular anion	(6,3) network	(4,4) network	ribbon of juxtaposed squares
CCDC number	1505909	1505910	1505911

Structure	**1·2b·3a**	**1·2b·3b**	**1·2b·3c**	**1·2b·3d**
Formula	$C_{42}H_{72}Br_2F_{12}I_6N_4Na_2O_{12}$	$C_{42}H_{81.40}Br_2F_{17.73}I_{4.43}N_4Na_2O_{13.57}$	$C_{60}H_{90}Br_2F_{36}I_6N_4Na_2O_{15}$	$C_{60}H_{72}Br_2F_{48}I_6N_4Na_2O_{12}$
Molecular formula	2(**1·2b**)·3(**3a**)	2(**1·2b**)·2.217(**3b**)· 0.783(**EtOH**)	2(**1·2a**)·3(**3c**)·3(**EtOH**)	2(**1·2a**)·3(**3d**)
Fw	2020.24	2036.81	2758.56	2920.42
Crystallographic System	Trigonal	Monoclinic	Trigonal	Triclinic
Space group	*R*-3*c*	*Cc*	*R*-3	***P***-1
a (Å)	11.5113(14)	19.7905(15)	11.4448(15)	11.4362(12)
b (Å)	11.5113(14)	11.4577(9)	11.4448(15)	11.5407(12)
c (Å)	84.749(10)	32.498(2	58.475(8)	20.084(2)
α (°)	90	90.00	90	88.409(10)
β (°)	90	97.627(10)	90	89.682(11)
γ (°)	120	90.00	120	60.533(8)
V (Å^3)	9726(2)	7303.8(9)	6633.1(15)	2306.8(4)
T (K)	103	103	103	103
Z	6	4	3	1
ρ (g.cm^{-3})	2.070	1.852	2.072	2.102
μ (mm^{-1})	4.209	3.096	3.156	3.047
Absorption correction T_{min}, T_{max}	0.2317, 0.3824	0.4800, 0.5519	0.4380, 0.5769	0.6247, 0.6958

Collected, independent, obs. [$I>\sigma(I)$] reflections	72173, 6612, 5687	148452, 30684, 26979	64013, 6979, 5994	67609, 12343, 8049
R_{int}	0.044	0.052	0.027	0.072
ϑ_{max}	40.11	35.07	36.52	29.23
Parameters, restraints	142, 45	323, 243	286,363	604,0
$wR(F^2)$, $R[F^2 > 2\sigma(F^2)]$	0.0585, 0.0268	0.0633, 0.0335	0.0875, 0.0315	0.0651, 0.0343
Goodness of fit	1.103	1.058	1.073	0.920
$\Delta\rho$ (min,max)	-1.4,1.3	-1.5,1.1	-0.9, 1.7	-0.8, 1.3
Topology of supramolecular anion	(6,3) network	(6,3) network	(6,3) network	pearl necklace
CCDC number	1505912	1505913	1505914	1505915

Table S.2. Crystallographic data and structure refinement parameters for cocrystals formed by crypt-222 (**1**), sodium iodide (**2c**), and α,ω-diiodoperfluoroalkanes **3c,d**. **1·2c·3a** Has already been published (*Acta Cryst.* **2013**, *E68*, m387-388; refcode: AFEHAW).

Structure	**1·2c·3c**	**1·2c·3d**
Formula	$C_{56}H_{78}F_{36}I_8N_4Na_2O_{13}$	$C_{60}H_{72}F_{48}I_8N_4Na_2O_{12}$
Molecular formula	2(**1·2c**)·3(**3c**)·**EtOH**	2(**1·2c**)·3(**3d**)
Fw	2760.40	3014.4
Crystallographic System	Monoclinic	Triclinic
Space group	*C*2/*c*	***P***-1
a (Å)	20.224(2)	11.6302(6)
b (Å)	11.5766(9)	11.6788(6)
c (Å)	38.451(3)	20.1421(10
α (°)	90	88.653(3)
β (°)	101.478(9)	88.965(2)
γ (°)	90	60.148(2)
V (Å^3)	8822.3(13)	2372.1(2)
T (K)	150	103
Z	4	1
ρ (g.cm^{-3})	2.078	2.110
μ (mm^{-1})	2.952	2.77
Absorption correction T_{min},T_{max}	0.4380, 0.5769	0.4240, 0.4939
Collected, independent, obs. [$I>\sigma(I)$] reflections	75607, 13172, 10265	134012, 14968, 1293
R_{int}	0.057	0.028
ϑ_{max}	30.55	31.09
Parameters, restraints	805, 1597	959, 1139
$wR(F^2)$, $R[F^2 > 2\sigma(F^2)]$	0.1452, 0.0623	0.1557, 0.0589
Goodness of fit	1.151	1.130
$\Delta\rho$ (min,max)	-3.1,1.5	-1.6, 3.4
Topology of supramolecular anion	(6,3) network	Borromean interpenetrated (6,3) network
CCDC number	1505916	1505917

Table S.3. Crystallographic data and structure refinement parameters for cocrystals formed by crypt-222 (**1**), potassium halides **2d-f**, and α,ω-diiodoperfluoroalkanes **3c-e**. **1·2f·3a**, **1·2f·3b**, **1·2f·3c**, and **1·2f·3d** have already been published (*Chem. Commun.* **2006**, 1819-1821; refcodes: TEHQUT, IHURAE, TEHRAA, and IHUQUX, respectively).

Structure	**1·2d·3c**	**1·2d·3d**
Formula	$C_{56}H_{78}Cl_2F_{36}I_6\ K_2N_4O_{13}$	$C_{60}H_{72}Cl_2F_{48}I_6\ K_2N_4O_{12}$
Molecular formula	2(**1·2d**)·3(**3c**)·**EtOH**	2(**1·2d**)·3(**3d**)
Fw	2609.72	2863.72
Crystallographic System	Monoclinic	Trigonal
Space group	$\boldsymbol{P}2_1/n$	***P***-3
a (Å)	12.876(2)	11.912(2)
b (Å)	22.489(4)	11.912(2)
c (Å)	15.665(3)	20.261(4)
α (°)	90	90
β (°)	100.51(2)	90
γ (°)	90	120
V (Å^3)	4460.0(14)	2489.8(6)
T (K)	90	127
Z	2	1
ρ (g.cm^{-3})	1.943	1.910
μ (mm^{-1})	2.371	2.149
Absorption correction $T_{\mathrm{min}}, T_{\mathrm{max}}$	0.6928, 1.0000	0.7541, 1.0000
Collected, independent, obs. [$I>\sigma(I)$] reflections	74973, 12998, 11656	25438, 3841, 3281
R_{int}	0.032	0.023
ϑ_{max}	30.00	27.49
Parameters, restraints	614, 20	304, 557
$wR(F^2), R[F^2 > 2\sigma(F^2)]$	0.1186, 0.0548	0.1257, 0.0530
Goodness of fit	1.113	1.040
Δρ (min,max)	-0.8,1.9	-0.6,1.2
Topology of supramolecular anion	ribbon of juxtaposed squares	Borromean interpenetrated (6,3) network
CCDC number	1505918	1505919

Structure	**1·2e·3c**	**1·2e·3d**	**1·2f·3e**
Formula	$C_{56}H_{78}Br_2F_{36}I_6K_2N_4O_{13}$	$C_{60}H_{72}Br_2F_{48}I_6\ K_2N_4O_{12}$	$C_{48}H_{36}F_{60}I_7KN_2O_6$
Molecular formula	2(**1·2e**)·3(**3c**)·**EtOH**	2(**1·2e**)·3(**3d**)	**1·2f**·3(**3e**)
Fw	2746.38	2952.64	2804.19
Crystallographic System	Monoclinic	Trigonal	Triclinic
Space group	$\boldsymbol{P}2_1$	***P***-3	***P***-1
a (Å)	12.897(2)	11.727(2)	13.976(2)
b (Å)	22.537(3)	11.727(2)	14.730(2)
c (Å)	16.022(2)	20.290(3)	21.282(3)
α (°)	90	90	100.10(2)
β (°)	99.657(16)	90	96.99(2)
γ (°)	90	120	102.38(2)
V (Å^3)	4591.0(11)	2416.5(5)	4154.8(10)
T (K)	103	127	193
Z	2	1	2
ρ (g.cm^{-3})	1.952	2.029	2.241
μ (mm^{-1})	2.952	2.986	2.843
Absorption correction $T_{\mathrm{min}}, T_{\mathrm{max}}$	0.4380, 0.5769	0.8498,1.0000	0.7366, 1.0000
Collected, independent,	75607, 13172, 10265	35618, 6464, 5316	92349, 23695, 12307

obs. [$I>\sigma(I)$] reflections			
R_{int}	0.057	0.027	0.039
ϑ_{max}	30.55	34.30	30.66
Parameters, restraints	805, 1597	329, 569	1467, 3269
$wR(F^2)$, $R[F^2 > 2\sigma(F^2)]$	0. 1469, 0.0627	0.0903, 0.0337	0.1908, 0.0604
Goodness of fit	1.150	1.099	0.911
$\Delta\rho$ (min,max)	-3.1,1.5	-0.9, 1.9	-1.4,3.0
Topology of supramolecular anion	ribbon of juxtaposed squares	Borromean interpenetrated (6,3) network	infinite chain of loosely connected discrete adducts
CCDC number	1505920	1505921	1505922

Table S.4. Crystallographic data and structure refinement parameters for cocrystals formed by crypt-222 (**1**), rubidium halides **2g-i**, and α,ω-diiodoperfluoroalkanes **3c,d**.

Structure	**1·2g·3c**	**1·2h·3c**	**1·2h·3d**
Formula	$C_{56}H_{78}Cl_2F_{36}I_6N_4O_{13}Rb_2$	$C_{54}H_{74}Br_2F_{36}I_6N_4O_{13}Rb_2$	$C_{60}H_{72}Br_2F_{48}I_6N_4O_{12}Rb_2$
Molecular formula	2(**1·2g**)·3(**3c**)**·EtOH**	2(**1·2h**)·3(**3c**)**·**H_2O	2(**1·2a**)·3(**3d**)
Fw	2702.46	2763.33	3045.38
Crystallographic System	Monoclinic	Triclinic	Trigonal
Space group	***P***$2_1/c$	***P***-1	***P***-3
a (Å)	18.3661(13)	20.402(6)	11.9008(12)
b (Å)	22.5367(16)	20.609(7)	11.9008(12)
c (Å)	22.0198(14)	21.141(7)	20.483(2)
α (°)	90	118.216(14)	90
β (°)	101.118(3)	118.520(14)	90
γ (°)	90	90.16(2)	120
V (Å^3)	8943.2(11)	6576(4)	2512.3(4)
T (K)	103	103	103
Z	6	3	1
ρ (g.cm^{-3})	2.007	2.093	2.013
μ (mm^{-1})	3.354	4.270	3.752
Absorption correction T_{min}, T_{max}	0.4380, 0.5769	0.5029, 0.5790	0.2548, 0.3463
Collected, independent, obs. [$I>\sigma(I)$] reflections	210518, 31976, 22078	75248, 25112, 13329	37410, 4335, 3286
R_{int}	0.054	0.091	0.035
ϑ_{max}	34.03	26.02	28.69
Parameters, restraints	1122, 391	1653, 1280	266, 428
$wR(F^2)$, $R[F^2 > 2\sigma(F^2)]$	0.0647, 0.0354	0.0939, 0.0562	0.2311, 0.0804
Goodness of fit	1.005	0.993	1.046
Δρ (min,max)	-1.1,1.4	-0.9, 1.0	-1.8, 5.7
Topology of supramolecular anion	ribbon of juxtaposed squares	Borromean interpenetrated (6,3) network	(6,3) network
CCDC number	1505923	1505924	1505925

Structure	**1·2i·3c**	**1·2i·3d**
Formula	$C_{54}H_{72}F_{36}I_8N_4O_{12}Rb_2$	$C_{60}H_{72}F_{48}I_8N_4O_{12}Rb_2$
Molecular formula	2(**1·2i**)·3(**3c**)	2(**1·2i**)·3(**3d**)
Fw	2839.30	3139.36
Crystallographic System	Trigonal	Trigonal
Space group	***P***-3	***P***-3
a (Å)	12.241(2)	12.0208(7)
b (Å)	12.241(2)	12.0208(7)
c (Å)	17.612(3)	20.2652(14)
α (°)	90	90
β (°)	90	90
γ (°)	120	120
V (Å^3)	2285.5(7)	2536.0(3)
T (K)	296	103
Z	2	1
ρ (g.cm^{-3})	2.063	2.056
μ (mm^{-1})	3.895	3.538
Absorption correction T_{min}, T_{max}	0.2592, 0.3667	0.2175, 0.3196
Collected, independent, obs. [$I>\sigma(I)$] reflections	29933, 1800, 1375	39814, 4955, 3853
R_{int}	0.040	0.030
ϑ_{max}	21.67	30.03

Parameters, restraints	233, 190	314, 487
$wR(F^2)$, $R[F^2 > 2\sigma(F^2)]$	0.1399, 0.0492	0.1633, 0.0582
Goodness of fit	1.040	1.048
$\Delta\rho$ (min,max)	-0.7,1.1	-1.7,3.1
Topology of supramolecular anion	Borromean interpenetrated (6,3) network	Borromean interpenetrated (6,3) network
CCDC number	1505926	1505927

Table S.5. Crystallographic data and structure refinement parameters for cocrystals formed by crypt-222 (**1**), ammonium halides **2j-l**, and α,ω-diiodoperfluoroalkanes **3a-d**.

Structure	**1·2j·3c**	**1·2j·3d**	**1·2k·3d**
Formula	$C_{56}H_{86}Cl_2F_{36}I_6N_6O_{13}$	$C_{60}H_{82}Cl_2F_{48}I_6N_6O_{13}$	$C_{60}H_{82}Br_2F_{48}I_6N_6O_{13}$
Molecular formula	**2(1·2j)·3(3c)·EtOH**	2(**1·2j**)·3(**3d**)·**H_2O**	**1·2k**·3(**3d**)
Fw	2567.6	2839.62	2928.54
Crystallographic System	Monoclinic	Trigonal	Trigonal
Space group	$P2_1/c$	*P*-3	*P*-3
a (Å)	18.272(2)	11.949(2)	11.9484(10)
b (Å)	22.620(3)	11.949(2)	11.9484(10)
c (Å)	22.105(3)	20.359(4)	20.449(2))
α (°)	90	90	90
β (°)	100.571(12)	90	90
γ (°)	90	120	120
V (Å^3)	8981(2)	2517.4(8)	2528.3(4)
T (K)	103	103	103
Z	4	1	1
ρ (g.cm^{-3})	1.899	1.861	1.923
μ (mm^{-1})	2.264	2.044	2.774
Absorption correction T_{min}, T_{max}	0. 3832, 0. 4986	0.5653, 0.6783	0.4074, 0.4923
Collected, independent, obs. [$I>\sigma(I)$] reflections	186042, 37032, 25785	44589, 4898, 3737	59789, 4382, 3093
R_{int}	0.044	0.037	0.032
ϑ_{max}	37.42	29.99	28.75
Parameters, restraints	805, 1597	212, 9	234, 89
$wR(F^2), R[F^2 > 2\sigma(F^2)]$	0.0668, 0.0343	0.1654, 0.0552	0.2638, 0.0778
Goodness of fit	1.001	1.066	1.030
Δρ (min,max)	-1.3,1.6	-0.9, 3.1	-1.0,1.9
Topology of supramolecular anion	ribbon of juxtaposed squares	Borromean interpenetrated (6,3) network	Borromean interpenetrated (6,3) network
CCDC number	1505928	1505929	1505930

Structure	**1·2l·3a**	**1·2l·3b**	**1·2l·3c**	**1·2l·3d**
Formula	$C_{44}H_{86}F_{12}I_8N_6O_{13}$	$C_{40}H_{40}F_{16}I_5N_3O_6$	$C_{54}H_{80}F_{36}I_8N_6O_{12}$	$C_{60}H_{80}F_{48}I_8N_6O_{12}$
Molecular formula	**2(1·2l)·3(3a)**	**1·2l·2(3b)**	**2(1·2l) ·3(3c)**	**2(1·2l) ·3(3d)**
Fw	2150.39	1429.11	2704.44	3004.50
Crystallographic System	Triclinic	Monoclinic	Tri gonal	Trigonal
Space group	*P*-1	*C*2/*m*	***P***-3	***P***-3_1c
a (Å)	13.6266(10)	14.369(3)	12.2742(3)	12.0821(3)
b (Å)	13.8928(10)	23.356(4)	12.2742(3)	12.0821(3)
c (Å)	19.4320(12)	13.780(3)	17.5343(5))	39.2838(10)
α (°)	99.707(3)	90	90	90
β (°)	94.565(4)	94.557(12)	90)	90
γ (°)	92.430(4)	90	120	120
V (Å^3)	3608.7(4)	4610.0(16)	2287.73(10)	4966.3(2)
T (K)	103	155	296	103
Z	2	4	1	2
ρ (g.cm^{-3})	1.979	2.059	1.963	2.009
μ (mm^{-1})	3.522	3.475	2.836	2.640
Absorption correction T_{min}, T_{max}	0.5236, 0.6131	0.2235, 0.3204	0.2526, 0.2956	0.4763, 0.5731
Collected, independent, obs. [$I>\sigma(I)$] reflections	132848, 19237, 12406	45579, 8224, 6428	25284, 2067, 1574	56452, 3981, 3098
R_{int}	0.053	0.035	0.051	0.052
ϑ_{max}	29.13	32.03	22.71	27.89

Parameters, restraints	896, 357	535, 306	238, 246	266, 428
$wR(F^2)$, $R[F^2 > 2\sigma(F^2)]$	0.0939, 0.0414	0.0804, 0.0367	0.1687, 0.0507	0.2083, 0.0687
Goodness of fit	1.007	1.116	1.084	1.067
$\Delta\rho$ (min,max)	-2.2,2.8	-1.6, 1.3	-0.5, 0.8	-2.0, 3.6
Topology of supramolecular anion	(6,3) network	Interpenetrated (4,4) network	Borromean interpenetrated (6,3) network	Borromean interpenetrated (6,3) network
CCDC number	1505931	1505932	1505933	1505934

S.3. NMR spectroscopy

Experiments aimed at establishing the most convenient conditions to synthesise the target library.

A) Assessment that cryptation occurs quite rapidly under adopted conditions.

Pure 4,7,13,16,21,24-hexaoxa-1,10-diazabicyclo[8.8.8]hexacosane (crypt-222, 1). ^{1}H NMR (400 MHz, Ethanol-*d₆*): δ, 3.70 (s, 12H) 3.63-3.66 (t, 12H), 2.71-2.73, (t, 12H).

Pure 1,2-diiodotetrafluoroethane (3a). ^{19}F NMR (400 MHz, Ethanol-d_6): δ, -57.71.

Pure 1,4-diiodooctafluorobutane (3b). ^{19}F NMR (400 MHz, Ethanol-d_6): δ, -65.11 (CF_2-I), -113.65 (CF_2CF_2-I).

Pure 1,6-diiodododecafluorohexane (3c). ^{19}F NMR (400 MHz, Ethanol-d_6): δ, -65.77 (CF_2-I), -113.65 (CF_2CF_2-I), -121.84 (CF_2 CF_2CF_2-I).

Pure 1,8-diiodohexadecafluorooctane (3d). ^{19}F NMR (400 MHz, Ethanol-d_6): δ, -66.01 (CF_2-I), -114.68 (CF_2CF_2-I), -121.79 (CF_2 CF_2CF_2-I), -122.68 (CF_2 CF_2 CF_2CF_2-I).

Solutions obtained on mixing 1, 2, and 3 in 1:1:1.5 ratio. The cryptand **1** (0.025 mmol), the halide salt **2** (0.025 mmol), and the α,ω-dioodoperfluoroalkane **3** (0.037 mmol) are added to an NMR tube containing ethanol-*d6* (0.5 mL) and the resulting system is monitored via ^{1}H and ^{19}F NMR. Spectra immediately after mixing of the starting tectons (Time 0) and after 12 hours at room temperature (Time 12) are reported.

Self-assembly in solutions formed starting from crypt-222 (1), sodium chloride (2a), and 1,2-diiodotetrafluoroethane (3a). Time 0: ^{1}H NMR (400 MHz, Ethanol-d_6): δ, 3.67 (s, 12H), 3.62-3.65 (t, 12H), 2.68-2.71, (t, 12H); ^{19}F NMR (400 MHz, Ethanol-d_6): δ -57.78. Time 12: ^{1}H NMR (400 MHz, Ethanol-d_6): δ, 3.64 (s, 12H) 3.62-3.64 (t, 12H), 2.68-2.70, (t, 12H); ^{19}F NMR (400 MHz, Ethanol-d_6): δ -57.78.

Self-assembly in solutions formed starting from crypt-222 (1), sodium bromide (2b), and 1,4-diiodooctafluorobutane (3b). Time 0: ^{1}H NMR (400 MHz, Ethanol-d_6): δ, 3.68 (s, 12H), 3.63-3.66 (t, 12H), 2.69-2.72, (t, 12H); ^{19}F NMR (400 MHz, Ethanol-d_6): δ -65.21, -113.64. Time 12: ^{1}H NMR (400 MHz, Ethanol-d_6): δ, 3.68 (s, 12H) 3.63-3.65 (t, 12H), 2.69-2.71, (t, 12H); ^{19}F NMR (400 MHz, Ethanol-d_6): δ -65.21, -113.64.

Self-assembly in solutions formed starting from crypt-222 (1), sodium iodide (2c), and 1,8-diiodohexadecafluorooctane (3d). Time 0: ^{1}H NMR (400 MHz, Ethanol-d_6): δ, 3.67 (s, 12H), 3.62-3.64 (t, 12H), 2.68-2.70, (t, 12H); ^{19}F NMR (400 MHz, Ethanol-d_6): δ -66.18, -114.69, -121.79, -

122.67. Time 12: ^{1}H NMR (400 MHz, Ethanol-*d$_6$*): δ, 3.67 (s, 12H) 3.62-3.64 (t, 12H), 2.68-2.70, (t, 12H); ^{19}F NMR (400 MHz, Ethanol-*d$_6$*): δ -66.18, -114.74, -121.85, -122.73.

Self-assembly in solutions formed starting from crypt-222 (1), rubidium bromide (2h), and 1,6-diiodododecafluorohexane (3c). Time 0: ^{1}H NMR (400 MHz, Ethanol-*d$_6$*): δ, 3.64 (s, 12H), 3.57-3.59 (t, 12H), 2.58-2.61, (t, 12H); ^{19}F NMR (400 MHz, Ethanol-*d$_6$*): δ -65.91, -114.67, -121.82. Time 12: ^{1}H NMR (400 MHz, Ethanol-*d$_6$*): δ, 3.64 (s, 12H) 3.57-3.59 (t, 12H), 2.58-2.60, (t, 12H); ^{19}F NMR (400 MHz, Ethanol-*d$_6$*): δ -65.91, -114.67, -121.82.

Self-assembly in solutions formed starting from crypt-222 (1), ammonium chloride (2j), and 1,8-diiodohexadecafluorooctane (3d). Time 0: ^{1}H NMR (400 MHz, Ethanol-*d$_6$*): δ, 6.98-7.24 (t, 4H), 3.65 (s, 12H), 3.59-3.61 (t, 12H), 2.59-2.61, (t, 12H); ^{19}F NMR (400 MHz, Ethanol-*d$_6$*): δ -66.08, -114.67, -121.78, -122.66, Time 12: ^{1}H NMR (400 MHz, Ethanol-*d$_6$*): δ, 3.65 (s, 12H) 3.58-3.61 (t, 12H), 2.59-2.61, (t, 12H), NH_4 protons were a very broad signal in the range 6.9 to 7.5 ; ^{19}F NMR (400 MHz, Ethanol-*d$_6$*): δ -65.07, -114.70, -121.83, -122.70.

B) Assessment that cocrystals with the same composition are formed independent of the stoichiometry and composition of starting solution.

Ethanol solutions obtained by dissolving:

b1) the cation⊂crypt-222 halide (**1·2**) and the diiodoperfluoroalkane **3** in 1:1.5 ratio;

b2) the cryptand **1**, the salt **2**, and the diiodoperfluoroalkane **3** in 1:1:1.5 ratio;

b3) the cryptand **1**, the salt **2**, and the diiodoperfluoroalkane **3** in 1:1:2 ratio;

b4) the cryptand **1**, the salt **2**, and the diiodoperfluoroalkane **3** in 1:1:1 ratio;

were slowly evaporated at room temperature. After 1-4 days the formed whitish crystals (25% ca. conversion) were filtered and analyzed via ^{1}H and ^{19}F NMR.

The following sets of starting materials were used:

crypt-222 (**1**), sodium chloride (**2a**), and 1,2-diiodotetrafluoroethane (**3a**);

crypt-222 (**1**), sodium bromide (**2b**), and 1,4-diiodooctafluorobutane (**3b**);

crypt-222 (**1**), sodium iodide (**2c**), and 1,8-diiodohexadecafluorooctane (**3d**);

crypt-222 (**1**), rubidium bromide (**2h**), and 1,6-diiodododecafluorohexane (**3c**);

crypt-222 (**1**), ammonium chloride (**2j**), and 1,8-diiodohexadecafluorooctane (**3d**).

^{1}H and ^{19}F NMR of cocrystals from solution b1) are reported below for the five sets of starting material. The same spectra were obtained for cocrystals afforded by solutions b2), b3), and b4), confirming that cocrystals with the same composition are formed independent of the stoichiometry and composition of starting solution.

Cocrystals formed starting from Na$^+$⊂crypt-222 chloride (1·2a) and 1,2-diiodotetrafluoroethane (3a). ^{1}H NMR (400 MHz, Ethanol-d_6): δ, 3.67 (s, 12H), 3.61-3.64 (t, 12H), 2.67-2.70, (t, 12H); ^{19}F NMR (400 MHz, Ethanol-d_6): δ -57.80.

Cocrystals formed starting from Na$^+$⊂crypt-222 bromide (1·2b) and 1,4-diiodooctafluorobutane (3b). ^{1}H NMR (400 MHz, Ethanol-d_6): δ, 3.67 (s, 12H), 3.62-3.64 (t, 12H), 2.68-2.70, (t, 12H); ^{19}F NMR (400 MHz, Ethanol-d_6): δ -65.20, -113.65.

Cocrystals formed starting from Na$^+$⊂crypt-222 iodide (1·2c) and 1,8-diiodohexadecafluorooctane (3d). ^{1}H NMR (400 MHz, Ethanol-d_6): δ, 3.67 (s, 12H), 3.62-3.64 (t, 12H), 2.68-2.70, (t, 12H); ^{19}F NMR (400 MHz, Ethanol-d_6): δ -66.14, -114.69, -121.78, -122.67.

Cocrystals formed starting from Rb$^+$⊂crypt-222 bromide (1·2h) and 1,6-diiodododecafluorohexane (3c). ^{1}H NMR (400 MHz, Ethanol-d_6): δ, 3.63 (s, 12H), 3.56-3.59 (t, 12H), 2.58-2.60, (t, 12H); ^{19}F NMR (400 MHz, Ethanol-d_6): δ -65.85, -114.68, -121.83.

Cocrystals formed starting from NH$_4^+$⊂crypt-222 chloride (1·2j) and 1,8-diiodohexadecafluorooctane (3d). ^{1}H NMR (400 MHz, Ethanol-d_6): δ, 3.65 (s, 12H), 3.58-3.61(t, 12H), 2.59-2.61, (t, 12H); ^{19}F NMR (400 MHz, Ethanol-d_6): δ -66.06, -114.68, -121.78, -122.67.

S.4. DSC analyses

Experiments aimed at establishing the most convenient conditions to synthesise the target library.

Assessment that the different solution stoichiometries and composition was not changing the formed cocrystal.

Thermal behaviors of all the complexes were established with a Mettler Toledo DSC600 hot stage (10 °C/min) under flowing nitrogen (flow rate 50 ml/min) using 50 µl sealed aluminum sample pans. The sealing was made by using a 30 µl aluminum pan with capillary holes as cover-pan to minimize a free volume inside a pan and to ascertain good thermal contact between sample and pan. Several heating/cooling cycles were performed to assess the reliability of the data; only one heating cycle (heating rate 10 °C/min) is reported here. DSC pictures for pure **1** and supramolecular cocrystals **1·2·3** are given below.

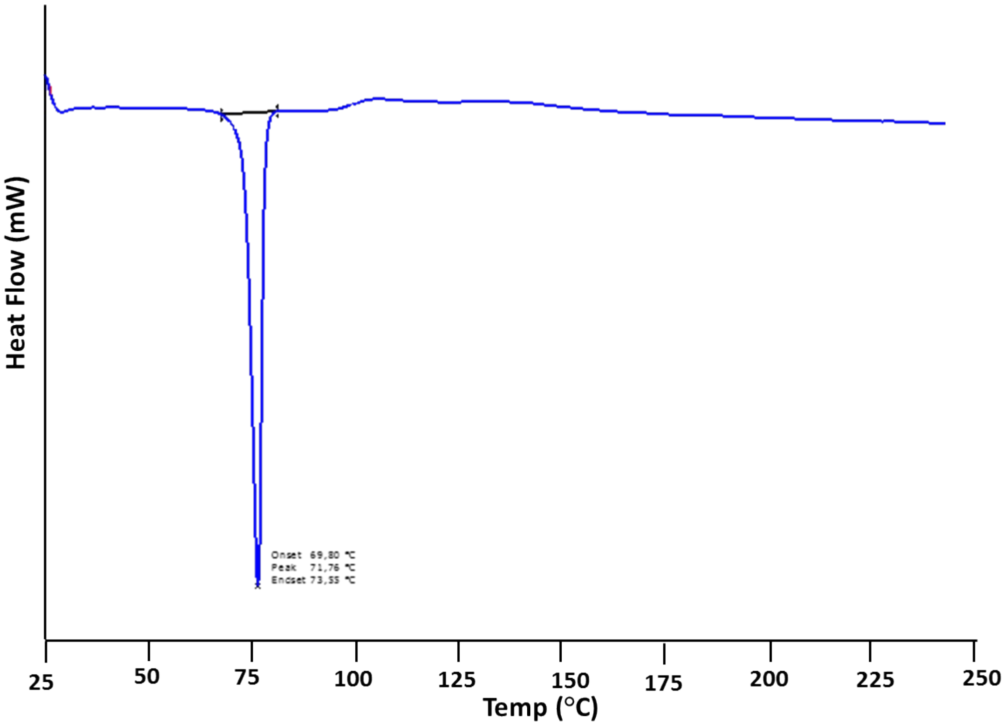

Figure S.1. DSC scan of pure crypt-222 **1** on heating (10 °C/min).

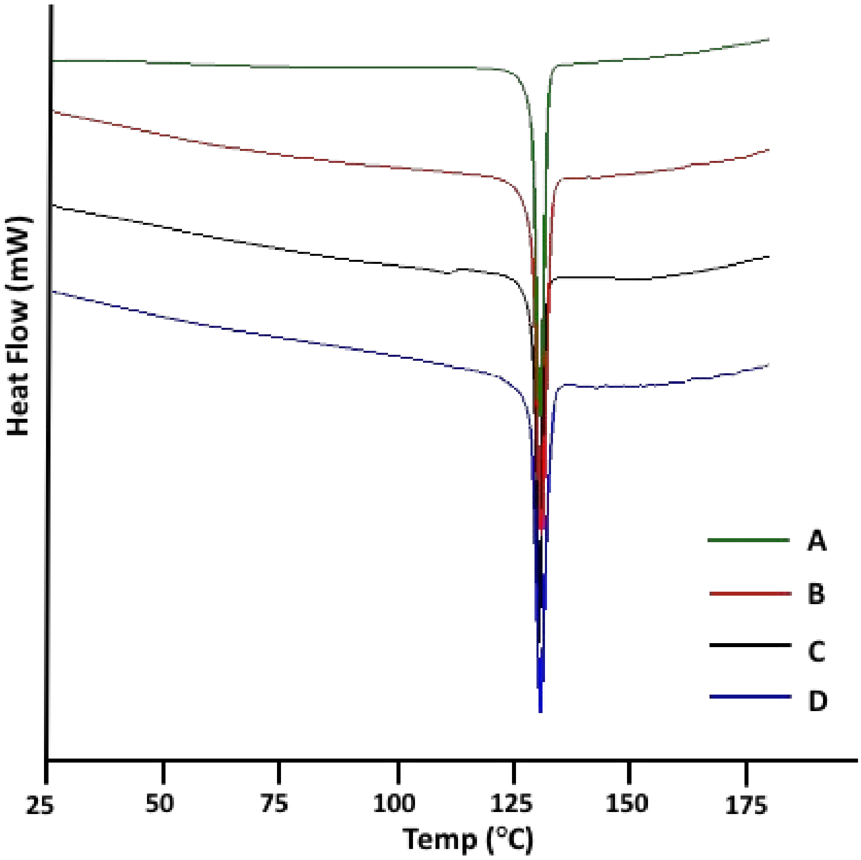

Figure S.2. Comparison of DSC thermograms of **1·2c·3d** obtained from solutions wherein **1**, **2c** and **3d** were present in different stoichiometric ratios: **(A)** 1:1:1.5 ratio; **(B)** 1:1:2 ratio; **(C)** 1:1:1 ratio; **(D)** cocrystals formed from solutions obtained on dissolving the preformed cryptated cation **1·2c** and **3d** in 1:1.5 ratio.

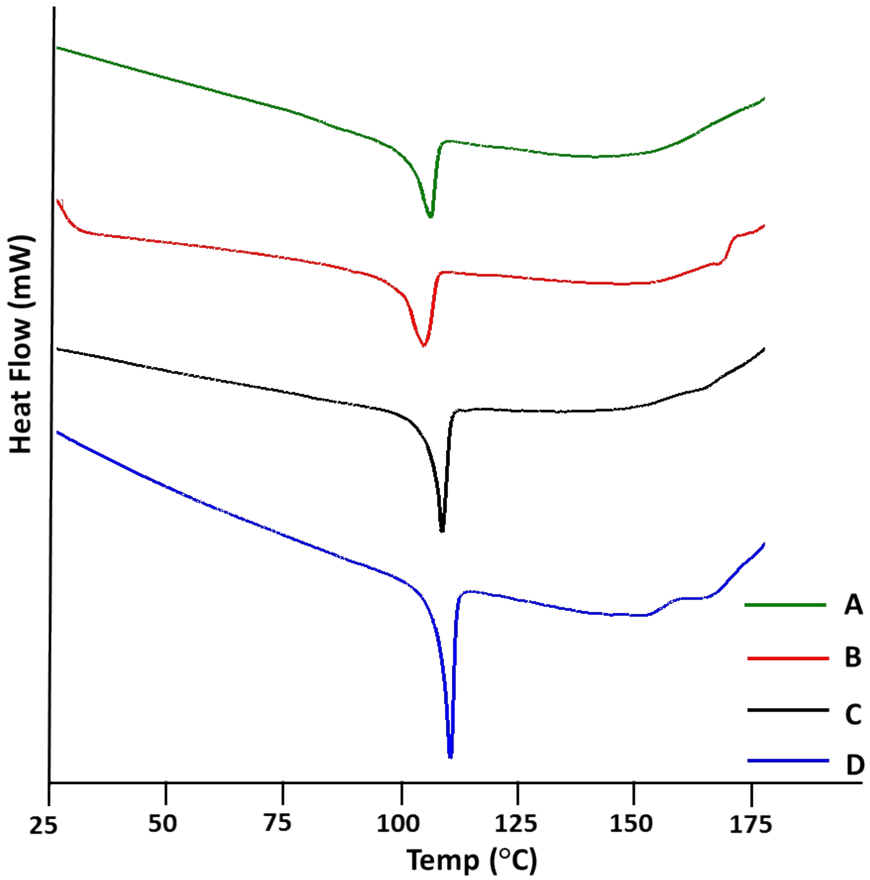

Figure S.3. Comparison of DSC thermograms of **1·2h·3c** obtained from solutions wherein **1**, **2h**, and **3c** were present in different stoichiometric ratios**: (A)** 1:1:1.5; **(B)** 1:1:2; **(C)** 1:1:1; **(D)** cocrystals formed from solutions obtained on dissolving the preformed cryptated cation **1·2h** and **3c** in 1:1.5 ratio.

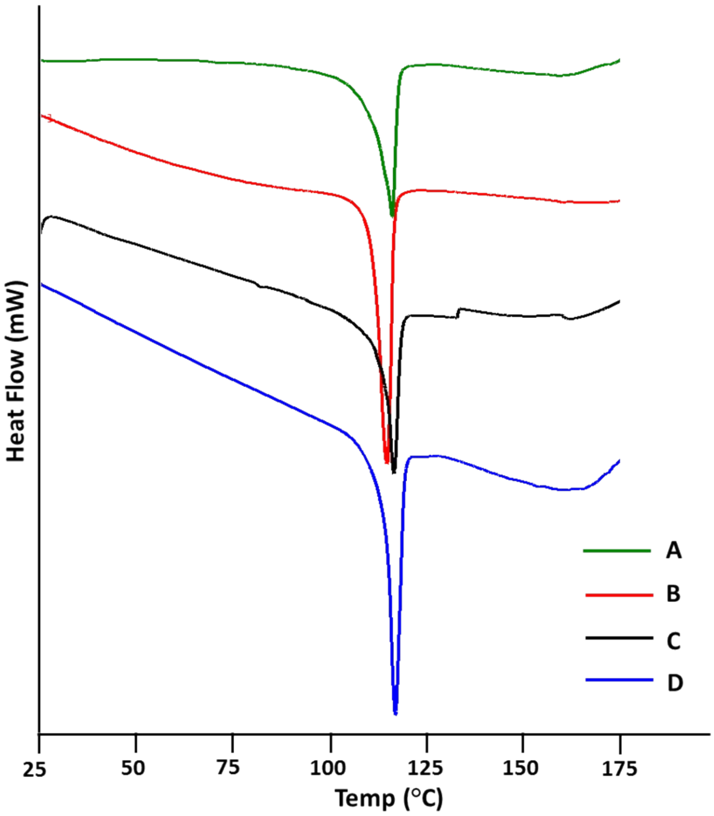

Figure S.4. Comparison of DSC thermograms of **1·2j·3d** obtained from solutions wherein **1**, **2j** and **3d** were present in different stoichiometric ratios**:** **(A)** 1:1:1.5; **(B)** 1:1:2; **(C)** 1:1:1; **(D)** cocrystals formed from solutions obtained on dissolving the preformed cryptated cation **1·2j** and **3d** in 1:1.5 ratio.

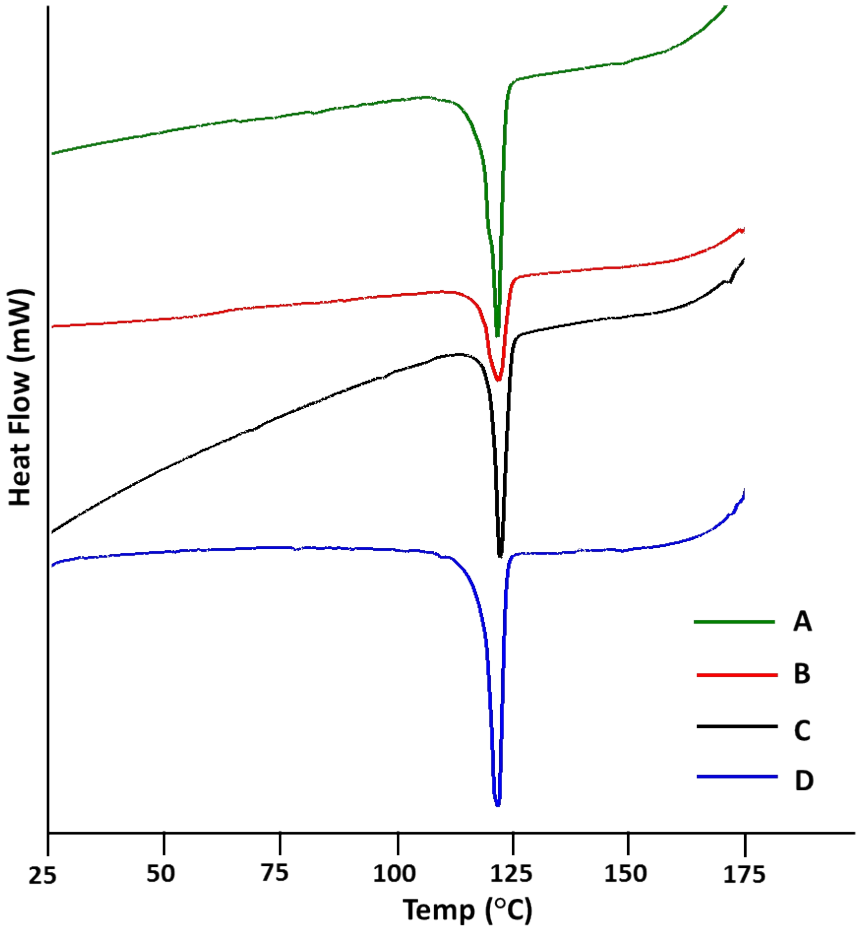

Figure S.5. Comparison of DSC thermograms of **1·2l·3c** obtained from solutions wherein **1**, **2l** and **3c** were present in different stoichiometric ratios**:** **(A)** 1:1:1.5; **(B)** 1:1:2; **(C)** 1:1:1; **(D)** cocrystals formed from solutions obtained on dissolving the preformed cryptated cation **1·2l** and **3c** in 1:1.5 ratio.

S.5. Powder X-Ray diffraction (PXRD) analyses

Experiments aimed at establishing the most convenient conditions to synthesise the target library.

Assessment that the used solution stoichiometry and composition was not changing the formed cocrystal.

Crystalline powder material of co-crystals were packed on borosilicate glass slides and the data sets were collected on Bruker D8 instrument at 293 K. The measurements were made in Bragg–Brentano geometry using Johansson monochromator to produce pure CuKα_1 radiation (1.5406 Å; 45kV, 30mA) and step–scan technique in 2θ range of 3.5–40°. The data were acquired from a spinning sample by X´Celerator detector in continuous scanning mode with a step size of 0.0167° using sample dependently counting times of 40 to 440 s per step. The experimental PXRD patterns of cocrystals and simulated patterns from the single crystal are shown below. The comparison of simulated and experimental PXRD pattern confirms the structural uniformity of bulk co-crystal powders. Few additional peaks (much weaker than the intensity gain of the main phase) are occasionally present in simulated patterns with respect to experimental patterns; this is probably related to some structural disorder and differences in data collection temperatures.

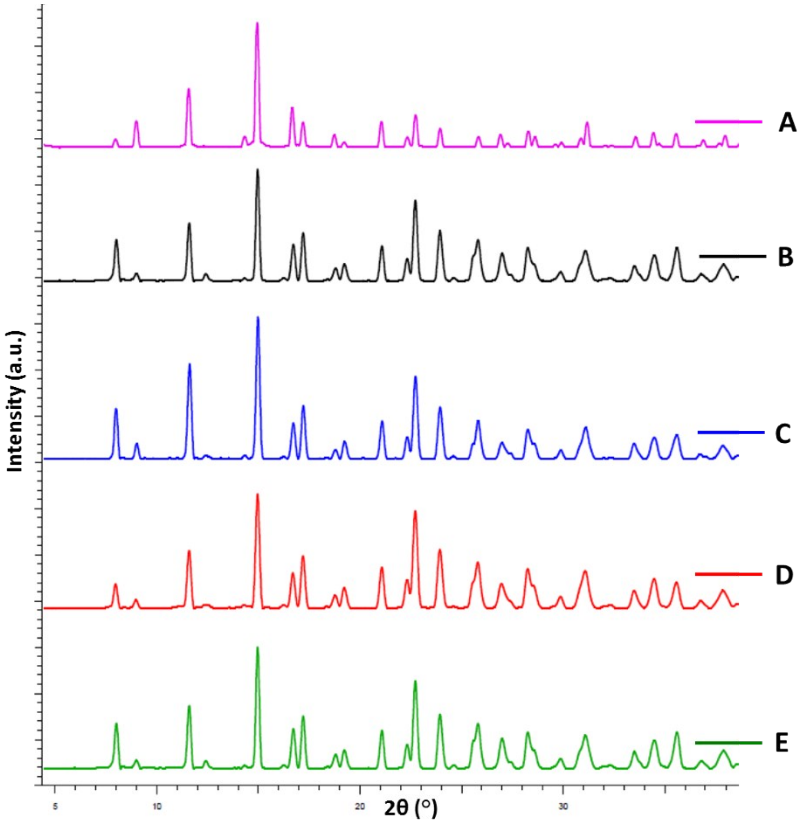

Figure S.6. Comparison of simulated and experimental PXRD patterns of **1·2c·3d** obtained using different experimental conditions: **(A)** Simulated powder pattern from single crystal structure (90 K); **(B)** Experimental pattern of cocrystals formed from solutions wherein **1**, **2c** and **3d** were present in 1:1:1.5 ratio; **(C)** Experimental pattern of cocrystals formed from solutions wherein **1**, **2c** and **3d** were present in 1:1:2 ratio; **(D)** Experimental pattern of cocrystals formed from solutions wherein **1**, **2c** and **3d** were present in 1:1:1 ratio; **(E)** Cocrystals formed starting from solutions obtained on dissolving the preformed cryptated cation **1·2c** and **3d** in 1:1.5 ratio.

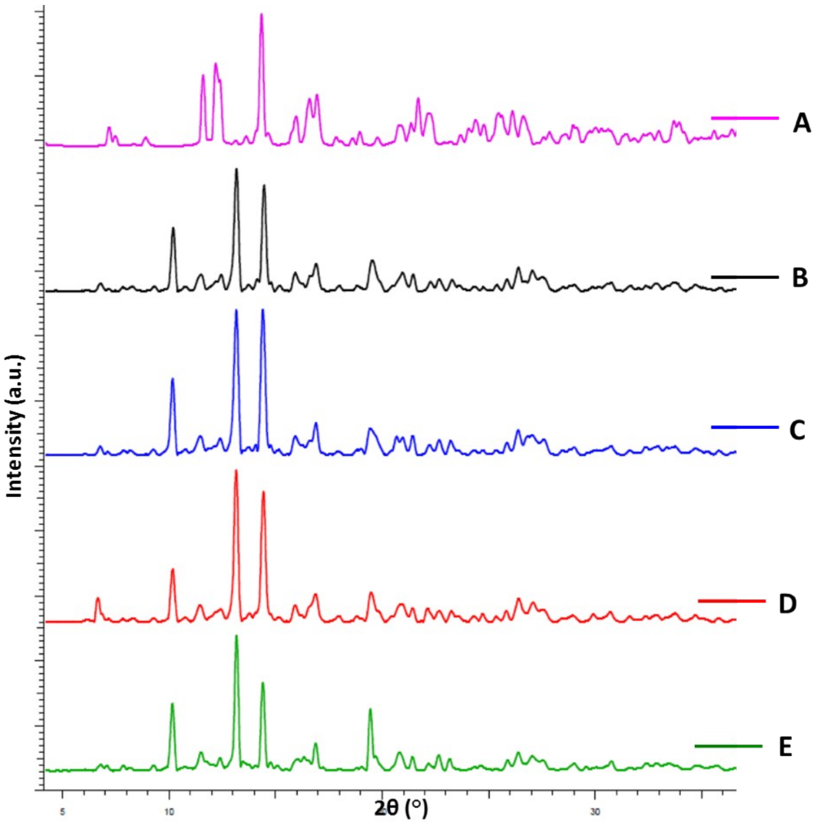

Figure S.7. Comparison of simulated and experimental PXRD patterns of **1·2h·3c** obtained using different experimental conditions: **(A)** Simulated powder pattern from single crystal structure (90 K); **(B)** Experimental pattern of cocrystals formed from solutions wherein **1**, **2h** and **3c** were present in 1:1:1.5 ratio; **(C)** Experimental pattern of cocrystals formed from solutions wherein **1**, **2h** and **3c** were present in 1:1:2 ratio; **(D)** Experimental pattern of cocrystals formed from solutions wherein **1**, **2h** and **3c** were present in 1:1:1 ratio; **(E)** Cocrystals formed starting from solutions obtained on dissolving the preformed cryptated cation **1·2h** and **3c** in 1:1.5 ratio

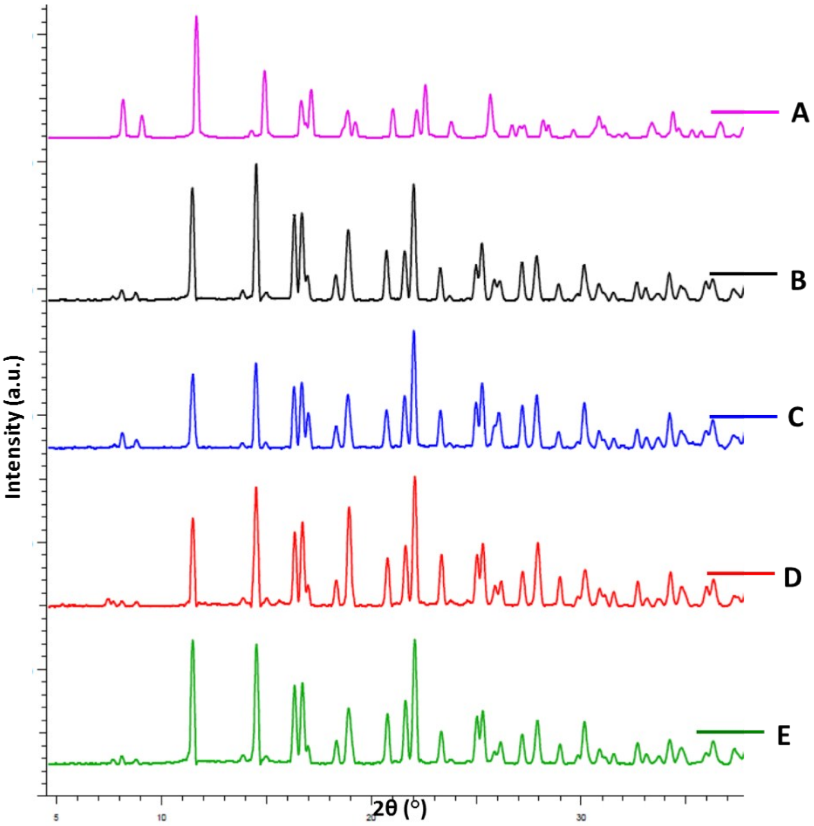

Figure S.8. Comparison of simulated and experimental PXRD patterns of **1·2j·3d** obtained using different experimental conditions:**:** **(A)** Simulated powder pattern from single crystal structure (90 K); **(B)** Experimental pattern of cocrystals formed from solutions wherein **1**, **2j** and **3d** were present in 1:1:1.5 ratio; **(C)** Experimental pattern of cocrystals formed from solutions wherein **1**, **2j** and **3d** were present in 1:1:2 ratio; **(D)** Experimental pattern of cocrystals formed from solutions wherein **1**, **2j** and **3d** were present in 1:1:1 ratio; **(E)** Cocrystals formed starting from solutions obtained on dissolving the preformed cryptated cation **1·2j** and **3d** in 1:1.5 ratio.

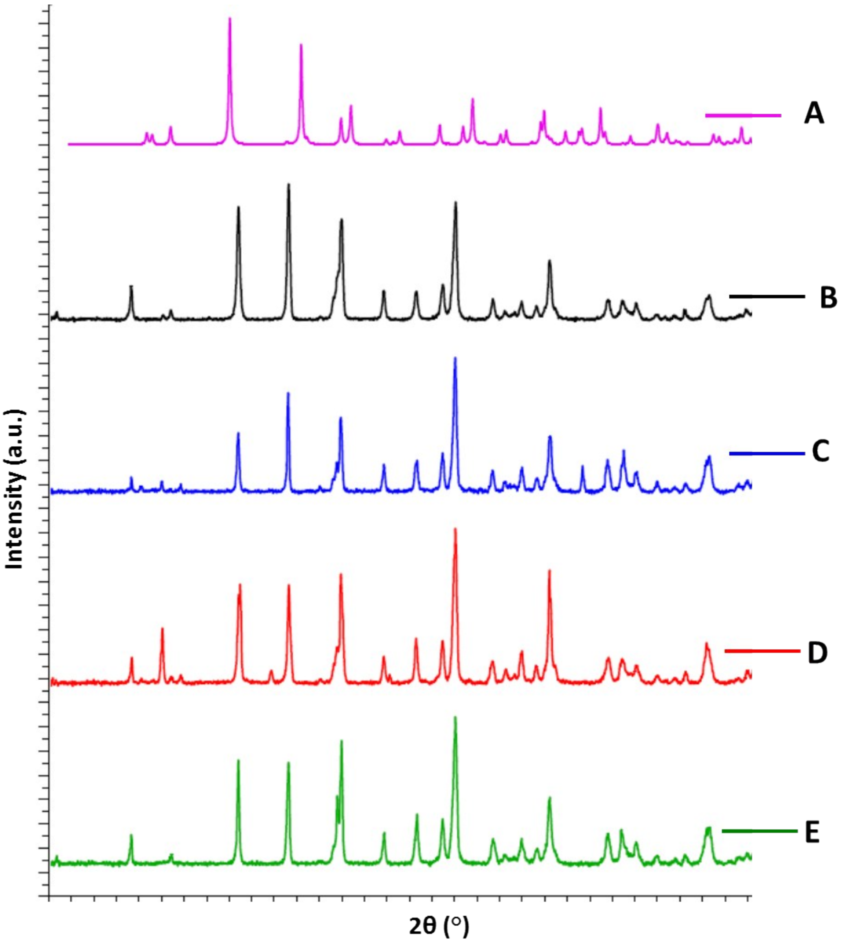

Figure S.9. Comparison of simulated and experimental PXRD patterns of **1·2l·3c** obtained using different experimental conditions: **(A)** Simulated powder pattern from single crystal structure (90 K); **(B)** Experimental pattern of cocrystals formed from solutions wherein **1**, **2l** and **3c** were present in 1:1:1.5 ratio; **(C)** Experimental pattern of cocrystals formed from solutions wherein **1**, **2l** and **3c** were present in 1:1:2 ratio; **(D)** Experimental pattern of cocrystals formed from solutions wherein **1**, **2l** and **3c** were present in 1:1:1 ratio; **(E)** Cocrystals formed starting from solutions obtained on dissolving the preformed cryptated cation **1·2l** and **3c** in 1:1.5 ratio.

S.6. IR analyses

Experiments aimed at establishing that fifty two halogen bonded cocrystals are obtained on crystallization of solutions containing 1, 2a-l, and 3a-e.

IR spectra were obtained using a Nicolet IS50 FT-IR spectrometer. Selected FTIR absorptions are reported. The XB driven cocrystal formation was proven by observed shifts of absorptions in cocrystals with respect to pure starting compounds.

Table S.6. Selected FTIR absorptions of starting tectons **1** and **3a-e** supramolecular cations **1·2a-l** and of cocrystals **1·2a-l·3a-e**. Shifts of observed absorptions in cocrystals with respect to pure starting compounds indicate the XB presence.

Compound	Frequency(cm^{-1})
1	2936, 2858, 2782, 1361, 1294
3a	1206, 1147, 1096
3b	1214, 1192, 1128
3c	1201, 1141, 1118
3d	1202, 1144, 1112
3e	1205, 1143, 1114

Compound	Frequency(cm^{-1})
1·2a	2967, 2879, 2820, 1360, 1304, 1263
1·2b	2966, 2874, 2816, 1360, 1304, 1263
1·2c	2956, 2857, 2806, 1355, 1300, 1260
1·2d	2960, 2884, 2814, 1355, 1295, 1259
1·2e	2958, 2884, 2812, 1354, 1295, 1259
1·2f	2963, 2858, 2815, 1357, 1290, 1262
1·2g	2957, 2882, 2812, 1352, 1296, 1258
1·2h	2957, 2881, 2810, 1351, 1295, 1258
1·2i	2956, 2873, 2819, 1349, 1294, 1258
1·2j	2960, 2882, 2811, 1359, 1296, 1258
1·2k	2964, 2878, 2809, 1358, 1301, 1260
1·2l	2968, 2877, 2812, 1359, 1296, 1259

Compound	Frequency(Cm^{-1})
1·2a·3a	2960, 2884, 2803, 1356, 1299, 1130, 1083
1·2a·3b	2973, 2865, 2814, 1353, 1299, 1185, 1115
1·2a·3c	2967, 2874, 2824, 1356, 1299, 1140, 1079
1·2a·3d	2973, 2884, 2824, 1356, 1302, 1130, 1075
1·2b·3a	2967, 2891, 2808, 1355, 1302, 1127, 1086

1·2b·3b	2972, 2889, 2816, 1358, 1301, 1186, 1120
1·2b·3c	2968, 2886, 2816, 1355, 1300, 1136, 1079
1·2b·3d	2971, 2889, 2824, 1355, 1300, 1140, 1105
1·2c·3a	2969, 2889, 2819, 1354, 1298, 1134, 1084
1·2c·3b	2969, 2892, 2820, 1358, 1301, 1187, 1120
1·2c·3c	2965, 2872, 2816, 1358, 1301, 1197, 1133
1·2c·3d	2968, 2892, 2819, 1358, 1301, 1140, 1112
1·2c·3e	2971, 2886, 2824, 1355, 1302, 1140, 1112
1·2d·3a	2960, 2884, 2813, 1355, 1298, 1139, 1097
1·2d·3b	2964, 2886, 2817, 1356, 1283, 1183, 1124
1·2d·3c	2966, 2883, 2813, 1353, 1298, 1136, 1079
1·2d·3d	2968, 2888, 2821, 1356, 1301, 1149, 1102
1·2d·3e	2967, 2887, 2819, 1354, 1301, 1152, 1102
1·2e·3a	2973, 2884, 2803, 1354, 1300, 1130, 1102
1·2e·3b	2974, 2886, 2814, 1355, 1301, 1187, 1121
1·2e·3c	2969, 2888, 2825, 1362, 1302, 1144, 1077
1·2e·3d	2969, 2885, 2822, 1363, 1301, 1150, 1103
1·2e·3e	2968, 2886, 2821, 1353, 1300, 1149, 1102
1·2f·3a	2971, 2864, 2801, 1362, 1300, 1133, 1085
1·2f·3b	2974, 2866, 2819, 1363, 1301, 1186, 1126
1·2f·3c	2966, 2888, 2823, 1363, 1303, 1143, 1077
1·2f·3d	2972, 2886, 2820, 1363, 1302, 1149, 1104
1·2f·3e	2965, 2890, 2812, 1362, 1303, 1140, 1112
1·2g·3a	2963, 2878, 2810, 1353, 1294, 1125, 1091
1·2g·3b	2965, 2880, 2813, 1353, 1298, 1179, 1128
1·2g·3c	2958, 2881, 2818, 1350, 1204, 1132, 1074
1·2g·3d	2959, 2880, 2808, 1351, 1295, 1135, 1108
1·2h·3a	2953, 2880, 2816, 1352, 1296, 1134, 1081
1·2h·3b	2962, 2882, 2812, 1353, 1280, 1177, 1097
1·2h·3c	2965, 2886, 2814, 1358, 1298, 1145, 1081
1·2h·3d	2961, 2885, 2811, 1353, 1296, 1138, 1104
1·2i·3a	2954, 2881, 2815, 1350, 1291, 1101, 1084
1·2i·3b	2964, 2886, 2809, 1354, 1296, 1181, 1110
1·2i·3c	2964, 2885, 2822, 1353, 1297, 1142, 1082
1·2i·3d	2959, 2879, 2807, 1350, 1298, 1148, 1101
1·2j·3a	2996, 2874, 2806, 1357, 1296, 1094
1·2j·3b	2961, 2883, 2817, 1357, 1297, 1183, 1100
1·2j·3c	2960, 2876, 2814, 1351, 1299, 1136, 1073
1·2j·3d	2969, 2885, 2818, 1360, 1304, 1150, 1100
1·2k·3a	2960, 2882, 2819, 1357, 1296, 1082
1·2k·3b	2964, 2885, 2815, 1359, 1300, 1186, 1117
1·2k·3c	2967, 2893, 2822, 1360, 1304, 1130, 1074
1·2k·3d	2966, 2887, 2817, 1362, 1298, 1150, 1073
1·2l·3a	2963, 2883, 2815, 1358, 1299, 1083
1·2l·3b	2962, 2883, 2814, 1359, 1300, 1187, 1127
1·2l·3c	2966, 2890, 2812, 1360, 1304, 1134, 1082
1·2l·3d	2963, 2879, 2809, 1358, 1296, 1147, 1102

S.7. Single crystal X-ray representations

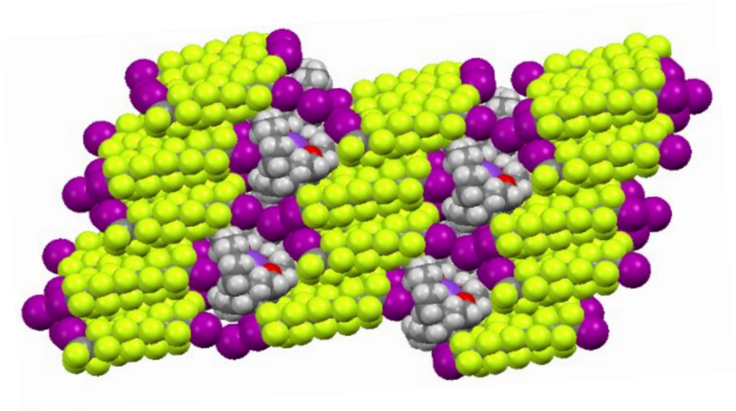

Figure S.10. Space filling representation (Mercury 3.8) of the overall crystal packing of **1·2f·3e** along the *b* axis showing the segregation of supramolecular anions. Color code: Grey, carbon; green, fluorine; purple, iodine.

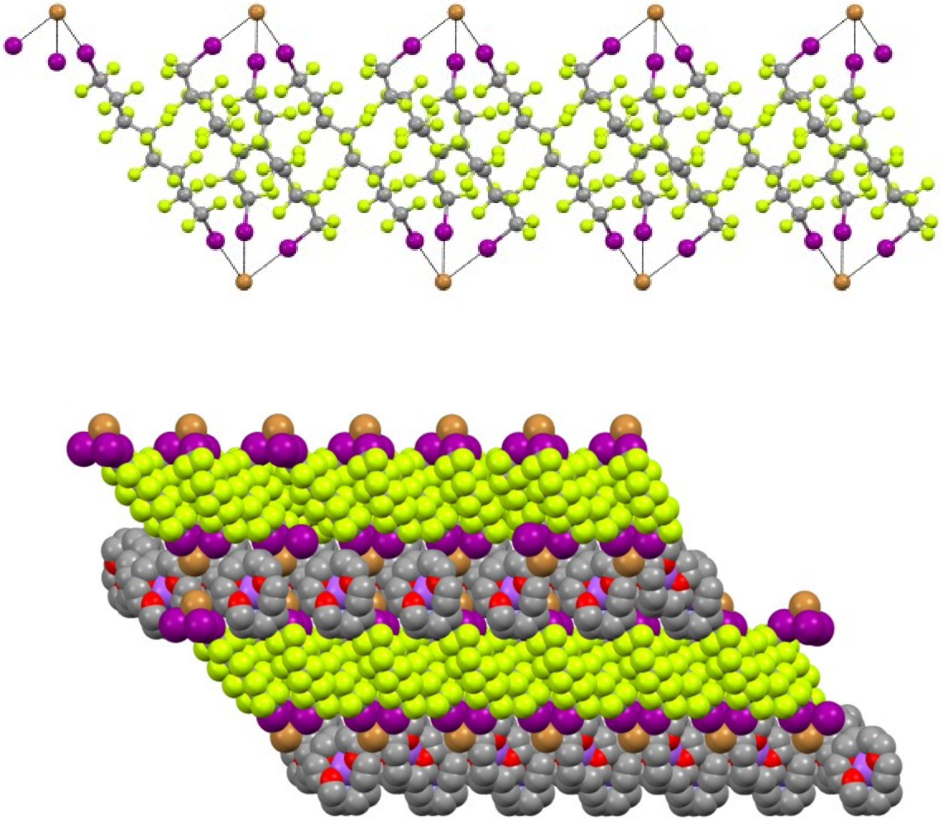

Figure. S.11. Representations (Mercury 3.8, along *a* axis) of cocrystal **1·2b·3d**. Top: fragment of a single necklace (in ball and stick) assembled via XB (dotted black lines). Bottom: alternating hydrocarbon and fluorous layers (in space filling) formed by supramolecular cations $Na^+\subset$crypt-222 and juxtaposed pearl-necklaces, respectively. Color codes: Grey, carbon; red, oxygen; violet, sodium; green, fluorine; purple, iodine; brown, bromine.

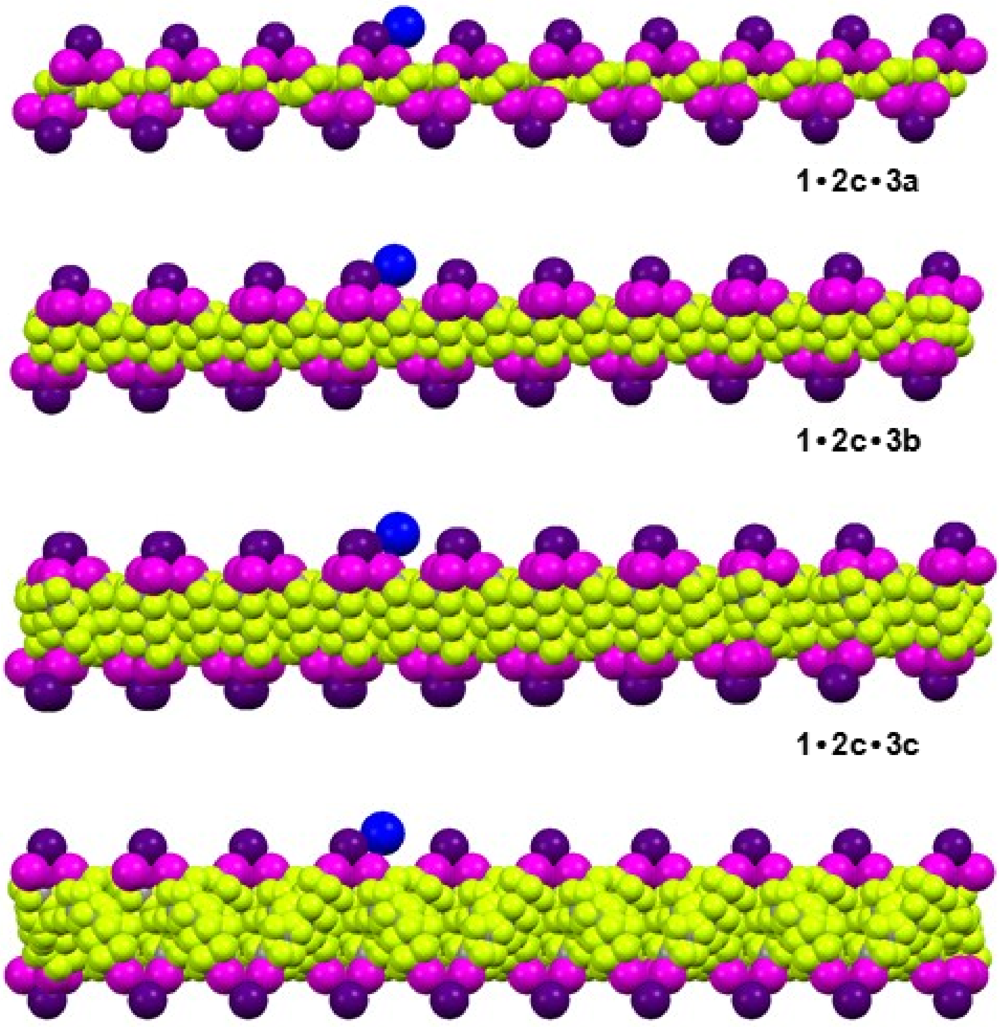

1•2c•3a

1•2c•3b

1•2c•3c

1•2c•3d

Figure. S.12. Space filling representation (Mercury 3.8, approximately along *a* axis) of the fluorous layers in cocrystals formed by **1**, sodium iodide (**2c**), and α, ω,-diodoperfluoroethane, -butane, -hexane, and -octane (**3a**, **3b**, **3c**, and **3d**, respectively). Only one Na$^+$ cation is represented, cryptand **1** has been omitted for sake of simplicity. Color codes: Green, fluorine; light purple, neutral iodine; dark purple, iodide anion; blue, sodium cation.

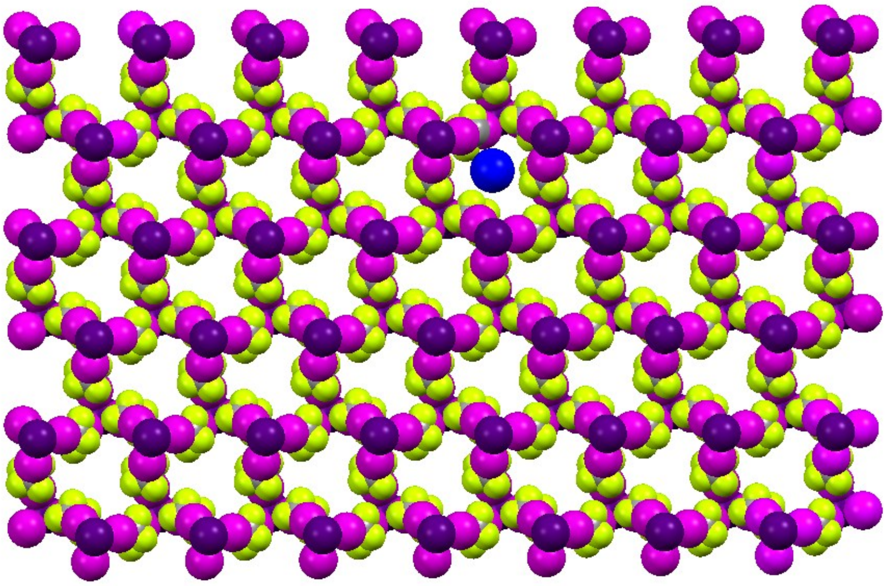

Figure S.13. Space filling representation (Mercury 3.8) of one fluorinated layer of cocrystal **1·2c·3a** showing how it shapes up as a (6,3) net; one supramolecular cation (crypt-222 ⊂ Na^+) is depicted as the sodium species only. Colours are as follows: blue, sodium cation; violet, iodide anion; magenta, neutral iodine; green, fluorine; grey, carbon; violet, potassium

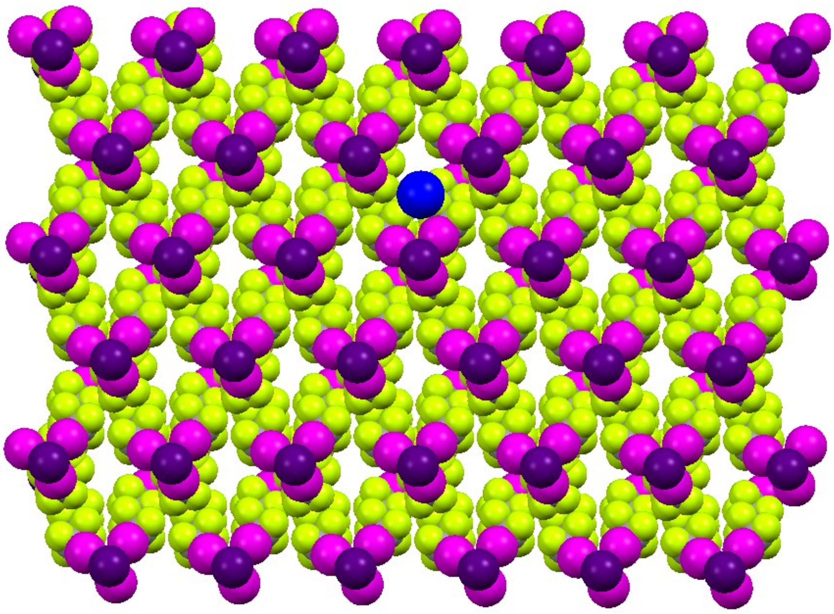

Figure S.14. Space filling representation (Mercury 3.8) of one fluorinated layer of cocrystal **1·2c·3b** showing how it shapes up as a (6,3) net; one supramolecular cation (crypt-222 ⊂ Na^+) is depicted as the sodium species only. Colours as in Fig. S.12.

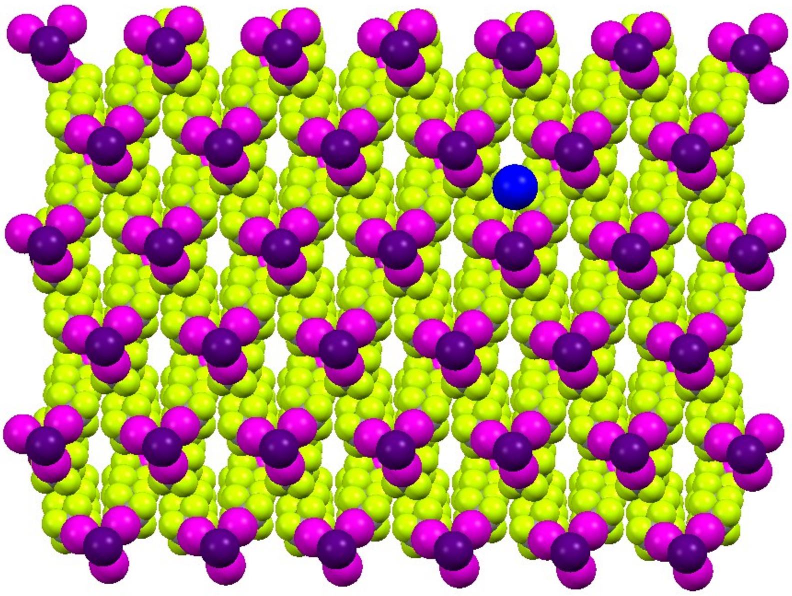

Figure S.15. Space filling representation (Mercury 3.8) of one fluorinated layer of cocrystal **1·2c·3c** showing how it shapes up as a (6,3) net; one supramolecular cation (crypt-222 ⊂ Na^+) is depicted as the sodium species only. The pyramidal arrangement of diiodoperfluorohexane moiety around iodide anions results in an increased thickness of the fluorous layer compared to **1·2c·3a** and **1·2c·3b**, (Fig. S.11), namely a greater separation between the two triangles defined by the alternating I^- (Fig. 4 of the paper). Colours as in Fig. S.12.

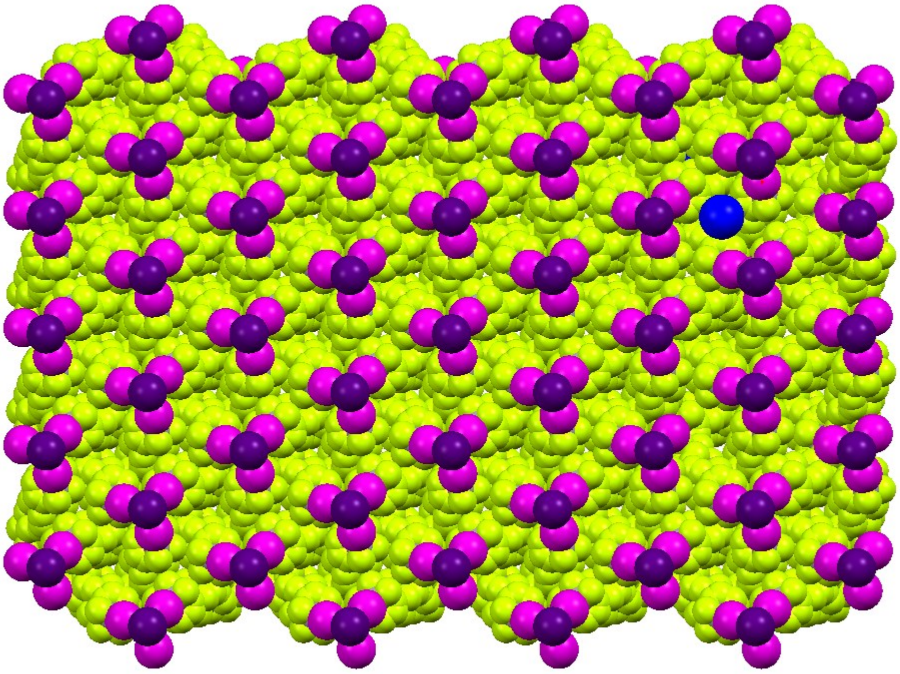

Figure S.16. Space filling representation (Mercury 3.8) of one fluorinated layer of cocrystal **1·2c·3d** showing how it shapes up as a (6,3) net; one supramolecular cation (crypt-222 ⊂ Na^+) is depicted as the sodium species only. The pyramidal arrangement of diiodoperfluorooctane moiety around iodide anions results in a thickness of the fluorous layer greater than in **1·2c·3a**, **1·2c·3b**, and **1·2c·3c**, (Fig. S.11), namely a greater separation between the two triangles defined by the alternating I^- (Fig. 4 of the paper). Colours as in Fig. S.12.

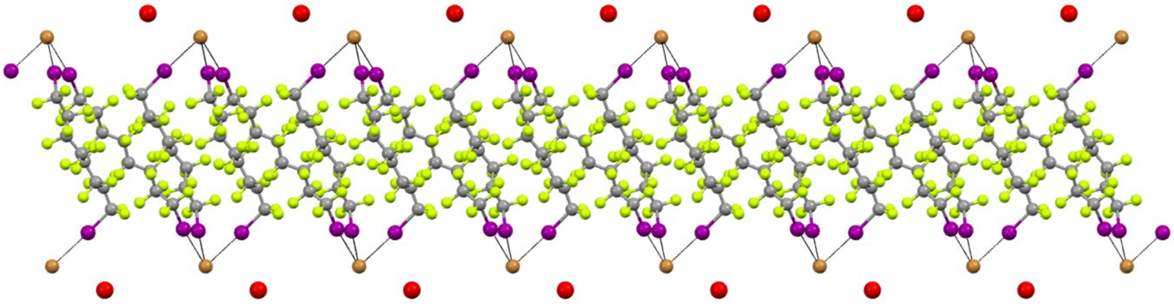

1·2b·3d

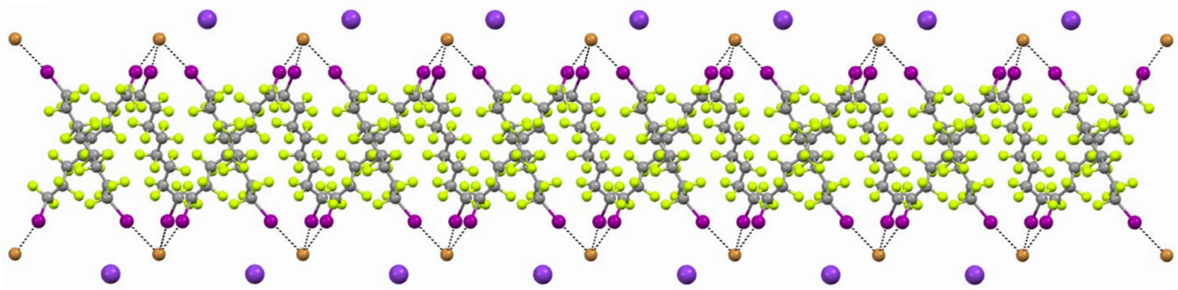

1·2e·3d

Figure S.17. Representation (Mercury 3.8, along the *a* axis) of one fluorous layer and adjacent cations of the crystal packing of pearl necklace **1·2b·3d** (top) and Borromean **1·2e·3d** (bottom) evidencing the structural similarity in the two cocrystals. For sake of simplicity cations are represented as sodium and potassium ions only. Color code: Grey, carbon; green, fluorine; purple, iodine; brown, bromine; red, sodium; violet, potassium.

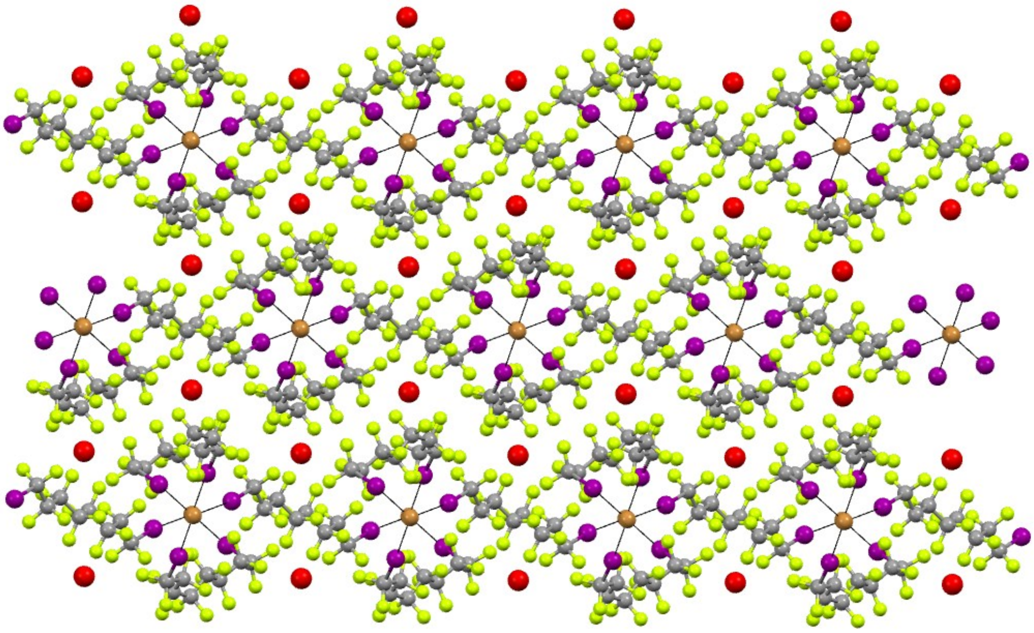

1·2b·3d

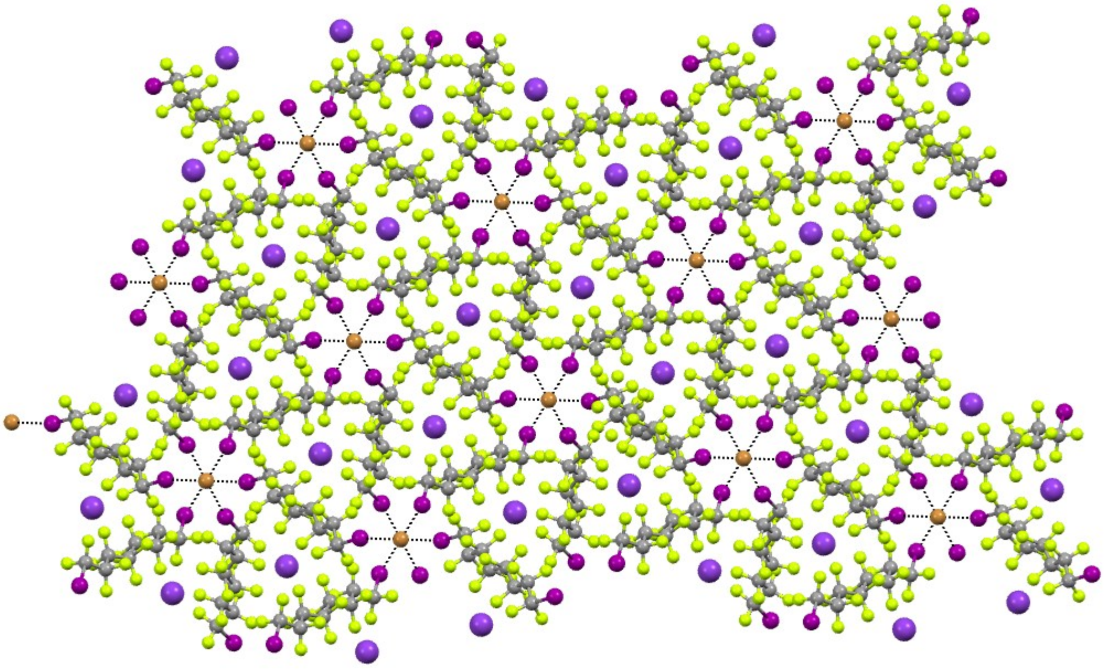

1·2e·3d

Figure S.18. Representation (Mercury 3.8, along the *c* axis) of one fluorous layer and adjacent cations of the crystal packing of the pearl necklace **1·2b·3d** (top) and the Borromean system **1·2e·3d** (bottom) evidencing the structural similarity in the two cocrystals. For sake of simplicity cations are represented as sodium and potassium ions only. Color code: Grey, carbon; green, fluorine; purple, iodine; brown, bromine; red, sodium; violet, potassium.

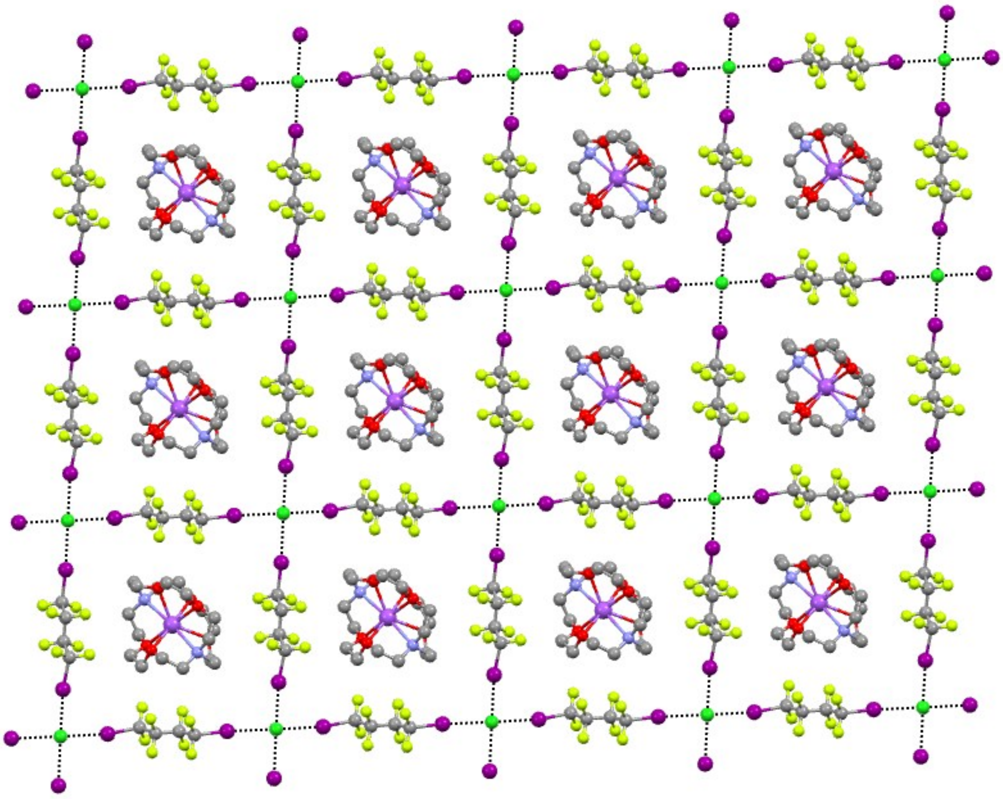

Figure S.19. Ball-and-stick representations (Mercury 3.8) of the (4,4) network formed in **1·2a·3b** by chloride anions, working as planar and tetradentate XB acceptors, and 1,4-diiodoperfluorobutane **3b**, working as node spacers. Cryptated sodium cations sit in the squares. XB are black dotted lines. Color code: Grey, carbon; light green, fluorine; green, chlorine; purple, iodine; red, oxygen; blue, nitrogen; violet, sodium.

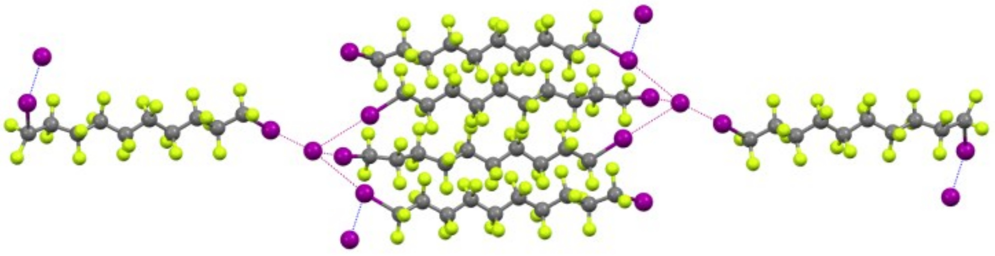

Figure S.20. Ball-and-stick representations (Mercury 3.8) of the well-defined supramolecular anion formed in **1·2f·3e** *via* interaction of two iodide anions with two diiodododecyl chains, which are bound to two iodide anions and bridge them, and with four other diiodododecyl chains, which are bound to one iodide anion. These supramolecular anions are assembled *via* fairly short XBs (red dotted lines, 343.6 – 360.7 pm, which correspond to normalized contacts (*Nc*) spanning 0.83 – 0.87). Color code: Grey, carbon; green, fluorine; purple, iodine.

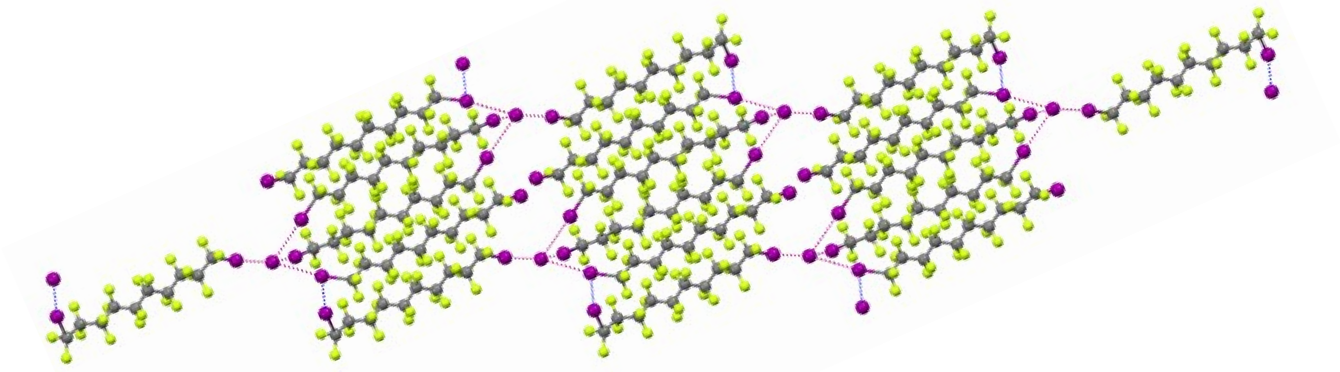

Figure S.21. Ball-and-stick representations (Mercury 3.8) of a part of the infinite array formed, approximately along the *c* axis, by long XBs (blue dotted lines, 373.7 pm, *Nc* = 0.90) connecting the supramolecular anions described in Fig. S.19. In these longer XBs the XB donors and acceptors sites are the positive cap and the negative belt of two iodine atoms of two diiodododecyl chains of the supramolecular anion described in Fig. S.19. Color code: Grey, carbon; green, fluorine; purple, iodine.

S.8. References

1. G.M. Sheldrick, *Acta Crystallogr. Sect. A.,* 2008, **64**, 112.

2. C. F. Macrae, I. J. Bruno, J.A. Chisholm, P. R. Edgington, P.McCabe, E. Pidcock, L. Rodriguez-Monge, R. Taylor, J. van de Streek, P. A. Wood, *J. Appl. Cryst.,* 2008, **41**, 466.

3. A. L. Spek, *Acta Crystallogr. Sect. D*, 2009, **65**, 148.